Excitation Enhancement of Hot Electrons by Ultrafast Optical Pumping in Heavily *p*-Doped Graphene Stacks

Yingying Zhu,[1] Jianan Wang,[1] Ru-Wen Peng,[1,*,§] Shiwei Wu,[2] Dongxiang Qi,[1,†,§] Wenzhong Bao,[3] Lianzi Liu,[1] Yi Zhu,[1] Hao Jing,[1] and Mu Wang[1,4,‡,§]

[1]*National Laboratory of Solid State Microstructures, School of Physics, and Collaborative Innovation Center of Advanced Microstructures, Nanjing University, Nanjing 210093, China*

[2]*State Key Laboratory of Surface Physics, Key Laboratory of Micro and Nano Photonic Structures (MOE), and Department of Physics, Fudan University, Shanghai 200433, China*

[3]*School of Microelectronics, Fudan University, 220 Handan Road, Shanghai 200433, China*

[4]*American Physical Society, Ridge, New York 11961, USA*

Energetic photoinduced hot electrons have been attracting increased scientific attention owing to their potential applicability in numerous photoelectrical and photochemical processes. Normally, the energy of electrons quickly converts into heat by ultrafast cooling, which is considered as the bottleneck for high-efficiency utilization of hot electrons. In this work, we explore intentionally heavily *p*-doped graphene stacks by degenerate femtosecond pump-probe spectroscopy, and observe an excitation enhancement of hot electrons at weak pump fluence. The time scale of hot-electron excitation is of the same order as that of fast decay via electron-electron and electron-optical-phonon scattering in our experiments. Physically, both Auger processes and population inversion are suppressed in this system, yet it becomes possible for the conduction bands to be effectively evacuated within the pulse duration through the ultrafast cooling of hot electrons, which may lead to an enhanced excitation of hot electrons. This excitation enhancement can be further strengthened by multiple layer-stacking processes or a thermal annealing pretreatment. The optical absorption of graphene stacks increases correspondingly, exhibiting a value larger than the linear limit at low pump fluence. Furthermore, the absorption modulation depth can reach approximately 0.79% in monolayer graphene for a small pump-fluence change (< 20 μJ/cm^2), further increasing to approximately 1.2% and approximately 2.5% in double- and triple-stacking graphene layers, respectively, indicating that the absorption can be sufficiently altered by an extremely small variation of pump fluence. These outcomes can be applied for low-cost pulse operations. We suggest that this effect can have potential applications to harvesting energy from excited hot electrons, and may provide a unique way to achieve high-speed modulators, photodetectors, solar cells, and photocatalysts.

I. INTRODUCTION

Electrons are considered to be hot if their energies are larger than thermal excitations at ambient temperatures [1]. The collection and utilization of hot electrons can stimulate enormous far-reaching physical or chemical processes and applications. For example, hot-carrier solar cells can harvest any photon energy that exceeds the semiconductor band gap to achieve high photoconversion efficiency [2,3]. Additionally, hot electrons can overcome tunnel barriers and be harnessed to enhance photocurrent and photovoltage performance through the excitation of surface plasmons [4–7]. Moreover, plasmon-induced

energetic hot carriers can facilitate chemical reactions or trigger photocatalysis processes with high throughput and low energy requirements [8,9]. Typically, the ultrafast cooling of hot electrons subsequent to excitation hinders the high-efficiency extraction and utilization of hot electrons [1,10], being an inevitable problem that limits the performance of hot-electron devices. Much effort has been devoted to slowing the relaxation of hot electrons to overcome the energy-loss problems [11,12].

On the other hand, two-dimensional (2D) materials offer a more effective means for stable, tunable, flexible, and integrated applications. Since the first fabrication of a single layer of graphene in 2004 [13,14], 2D materials have become one of the most extensively studied classes of materials owing to the wealth of unprecedented electrical, mechanical, thermal, and optical properties [15–17]. In the context of capturing hot electrons, strong light-matter interactions induced by these atomically thin materials

*rwpeng@nju.edu.cn
†dxqi@nju.edu.cn
‡muwang@nju.edu.cn
§To whom all correspondence (inquiry) should be addressed

provide a desirable platform for alternative hot-electron devices, such as a dual-gated bilayer graphene hot-electron bolometer [18], an intriguing structural phase transition in MoS_2 monolayer [19], plasmon-driven chemical reactions in graphene-Ag hybrids [20], and ultrafast plasmonic hot-electron transfer in Au nanoantenna/MoS_2 heterostructures [21]. Especially for graphene, angle-resolved photoemission spectroscopy and ultrafast pump-probe spectroscopy enable new levels of understanding and control of hot electrons down to the femtosecond time scale [22–27]. In pump-probe spectroscopy, the presence of pumped hot electrons alters the complex index of refraction of a graphene sample, and their dynamics can be detected by the time-delayed probe pulses with respect to the pump pulses [28–33].

The remarkable gapless and linear band structure of graphene opens up alternative carrier relaxation channels. For example, Auger scattering changes the number of charge carriers in the conduction band and gives rise to carrier multiplication [23,25,26]. And the ultrafast optical-phonon scattering results in an accumulation of carriers in the conduction band and a population inversion [22,27]. These have highlighted the fascinating and complex characteristics of the carrier dynamics in graphene. Recently, an unconventional double-bended saturation of carrier occupation has also been presented that has been ascribed to many-particle interactions [34,35]. So far, the carrier dynamics of graphene has been widely discussed both in theory and experiment, where the excitation process of hot electrons is mostly considered to be independent of their cooling process in graphene even with long-pulse excitation.

In this work, we report an experimental observation of the enhanced excitation of hot electrons in heavily p-doped graphene stacks with ultrafast weak optical pumping, where both carrier multiplication and population inversion are intentionally suppressed. By directing a femtosecond laser beam on the sample, electrons are pumped to the empty conduction bands with high energies while the pump pulse is present. These hot electrons transfer energy through electron-electron and electron-phonon scattering, cool down, and then evacuate the conduction bands. Our degenerate femtosecond optical pump-probe spectroscopy demonstrates that the time scale for electron excitation (which is equal to the pulse duration of $\tau_p \sim 137$ fs) is of the same order as that of fast electron cooling via electron-electron and electron-optical-phonon scattering. Thus, it is possible for the conduction bands to be effectively evacuated through the ultrafast cooling of hot electrons, which eventually results in an enhanced excitation of hot electrons. This excitation enhancement can be further strengthened by applying a multiple layer-stacking process or thermal annealing pretreatment. Additionally, the observed phenomena lead to an increased optical absorption of graphene stacks. Moreover, the absorption

modulation depth can reach approximately 0.79% for a small change of pump fluence (< 20 $\mu J/cm^2$), and further increase to approximately 1.2% and approximately 2.5% after stacking of more graphene layers. We suggest that a similar ultrafast dynamic process may occur in other materials with a simple energy band scheme as well, which inspires the design and fabrication of high-speed functional hot-electron nano-devices.

II. EXCITATION ENHANCEMENT OF HOT ELECTRONS IN MONOLAYER GRAPHENE

Graphene is a single atomic layer of sp^2 hybridized carbon with a honeycomb lattice, and its carriers behave as massless Dirac fermions with linear dispersion near the Fermi level [13,14,36,37]. The unique gapless band structure gives rise to an extremely short cooling time and ultra-broad nonlinear absorption ranging from the visible to the infrared region. Here, we start from single-layer graphene (SG) transferred on a standard Si/SiO_2 substrate. To evaluate the chemical potential of SG, we fabricate a typical liquid-electrolyte-based transistor with graphene, schematically shown in Fig. 1(a). The polymer applied is lithium perchlorate ($LiClO_4$) dissolved in poly(ethylene oxide), mixed with methanol [marked with gray in Fig. 1(a)]. By controlling the gate voltage, the moving ions can form an electric double layer at the electrolyte/channel interface. Figure 1(a) also shows the source-drain current as a function of the gate voltage using standard two-probe measurement and a parameter analyzer (Keithley 2636b). The heavily positive Dirac point voltage at approximately 0.7 V suggests that our graphene samples are heavily p-doped (approximately 600 meV) [38,39].

As schematically illustrated in Fig. 1(b), the optically induced hot electrons cool down via scattering. The cooling process usually includes carrier-carrier scattering and carrier-phonon scattering [40–42]. To trace the carrier dynamics, femtosecond optical pump-probe measurements are employed [as shown in Fig. 1(c)]. Pump and probe pulses come from a Ti:sapphire mode-locked laser (Spectra-Physics Mai Tai HP) with a pulse repetition rate of 80 MHz and, particularly, both are centered at a wavelength of 800 nm. Samples are illuminated by tightly focused pump pulses, and are detected by a time-delayed probe pulse with the same wavelength. The transient differential reflection ($\Delta R/R_0$) spectrum is measured as a function of the delay time, which is defined as the arrival time of the probe pulse with respect to the pump pulse. All the measurements are carried out at room temperature.

Firstly, we explore the induced hot electrons of SG experimentally under different pump fluences. Figure 1(d) shows the measured transient differential reflection signal ($\Delta R/R_0$) of SG, with corresponding pump fluence increasing from 2.74 to 19.18 $\mu J/cm^2$. For each transient differential reflection spectrum, two distinct processes can
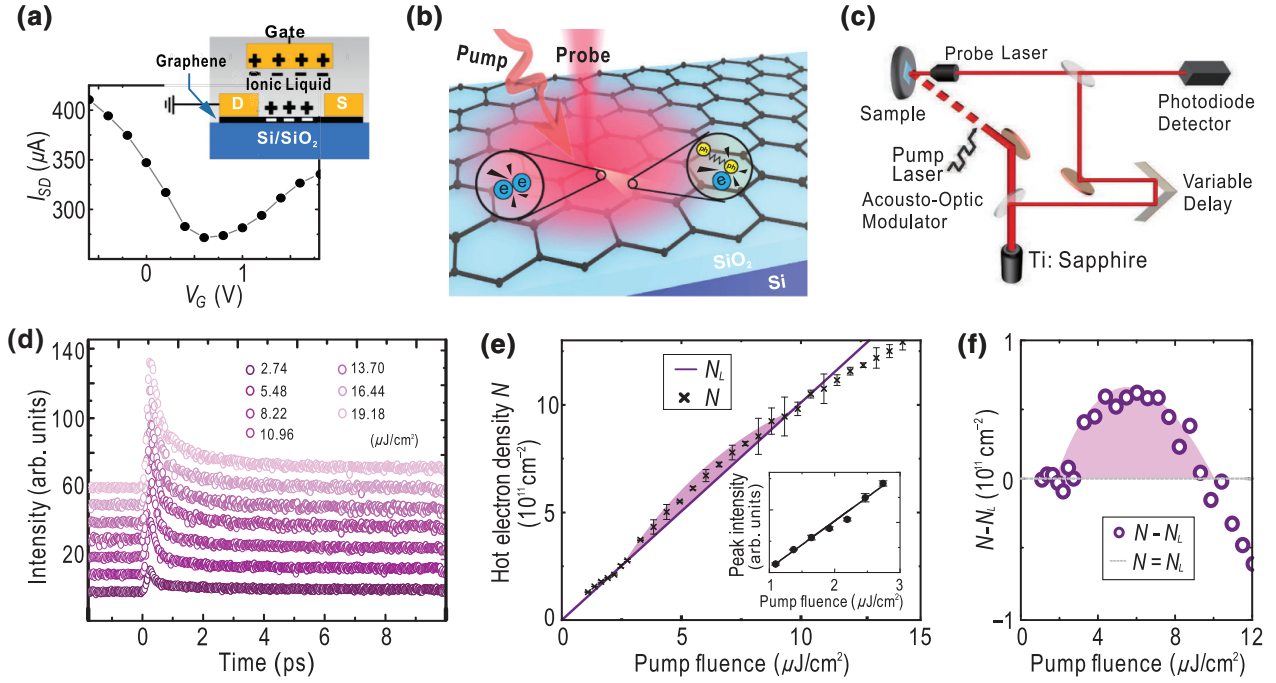
FIG. 1. (a) The measured source-drain current (I_{SD}) versus gate voltage (V_G) for SG with channel length of 50 μm. The source-drain voltage (V_{SD}) is 0.1 V. The inset is a schematic cross section of graphene electric-double-layer device with positive gate voltage. (b) Schematic illustration of monolayer graphene under ultrafast optical excitation. The optically induced hot electrons cool down via electron-electron scattering and electron-phonon scattering. (c) Schematic of the setup for our femtosecond optical pump-probe measurement. (d) Delay-time dependence of the normalized transient differential reflection spectra measured for SG, while increasing the pump power from 2.74 to 19.18 μJ/cm^2. The curves are shifted for clarity. (e) The deduced photoinduced hot electron density of SG from experimental data (black cross). The dark purple solid line represents the linear relation between N_L and pump fluence. The light purple area marks the region where $N > N_L$, as a guide to the eye. The inset shows the peak intensities of the measured signals in SG below 2.74 μJ/cm^2. (f) The differences of N (i.e., the density of photoinduced hot electrons) and its linear limit N_L with pump fluence. The light purple area marks the region where $N > N_L$, as a guide to the eye.

be identified: a rapid increase of the signal intensity followed by a significant decay of the signal intensity within a time scale of a few picoseconds. With increasing pump fluence, the signal intensity increases gradually. To estimate the excitation of hot electrons, we give a quantitative relationship between the density and peak intensity of $\Delta R/R_0$ as follows. For small signals, the reflective change is proportional to the absorptive change as [28]

$$\Delta R/R_0 \propto \Delta\alpha/\alpha_0. \tag{1}$$

The ultrafast absorptive change arises from the direct variations of the occupation number of graphene at the pump wavelength of 800 nm. Thus, the largest intensity of $\Delta R/R_0$ can in principle represent the maximum density of the excited hot electrons as [40,43,44]

$$N = k \times \Delta R/R_0, \tag{2}$$

where k is a constant. This linear relationship between $\Delta R/R_0$ and N is reasonable. This is because there is a linear relationship between the $\Delta R/R_0$ peak and the pump fluence when the pump fluence is lower than $I_0 =$

2.74 μJ/cm^2 [see the inset of Fig. 1(e)]. Based on this result, the density of the photoinduced hot electrons N can be quantitatively derived as a function of an excitation intensity I using

$$N(I) = N_0 \times \frac{\Delta R/R_0(I)}{\Delta R/R_0(I_0)}. \tag{3}$$

Here, $\Delta R/R_0(I)$ and $\Delta R/R_0(I_0)$ represent the peak intensities of the transient differential reflection with the corresponding pump fluence, and $N_0 = \alpha_0 \times I_0/\hbar\omega_{pump} = 2.77 \times 10^{11}$ cm^{-2} in the case for which every absorbed photon excites an electron at I_0, where $\hbar\omega_{pump} = 1.55$ eV and $\alpha_0 \cong 1.95\%$ based on the thin-film transmission formula [43,45].

As shown in Fig. 1(e), the density of photoinduced hot electrons (N) varies linearly as a function of the pump fluence for excitation intensities smaller than I_0, yet N exhibits a nonlinear relation when the pump fluence is further increased. However, it is noteworthy that within a certain range of the pump fluence, the density of hot electrons surpasses the corresponding linear limitation. To

better identify the increase of the density of photoinduced hot electrons (N) as a function of the pump fluence, we calculated the difference between N and its corresponding linear limitation (N_L) at each pump fluence [see Fig. 1(f)]. In Fig. 1(f), there is a region where $N > N_L$ (the light purple area), thus denoting an unusual enhancement of the excitation of hot electrons.

Normally, low-intensity excitation generates hot electrons in numbers proportional to the pump pulse energy (i.e., $N = N_L$), while high-intensity excitation creates large temporal populations of hot electrons in the conduction band. Accordingly, an additional absorption of incoming photons at the same energy will be forbidden according to the conduction-band-filling effect, thus giving rise to a reduction of the induced hot electrons (i.e., $N < N_L$). However, in our experiments, the value of N for photoinduced hot electrons is much higher than N_L within a certain pump fluence range after the linear region but before the band-filling region is reached. In other words, our data imply that the heating process of hot electrons becomes dependent on the cooling of the hot electrons.

It is noted that other nonlinear processes such as carrier multiplication and population inversion may cause an increase of hot electrons in graphene [22–24,29,46]. However, the carrier multiplication occurs only if impact ionization dominates over Auger recombination [23,27]. In the heavily p-doped graphene, the absence of electrons close to the Dirac point inhibits both impact ionization and Auger recombination [23,25], and hence the carrier multiplication process is suppressed. Meanwhile, the occurrence of population inversion demands strong optical pumping with a threshold pump fluence of approximately 200 μJ/cm^2 [27], which is much higher than the pump fluence ($<20 \mu$J/cm^2) in this work. Therefore, the observed excitation enhancement of hot electrons in our heavily p-doped graphene can be ascribed to neither carrier multiplication nor population inversion. We suggest the existence of another mechanism responsible for the excitation enhancement observed in our experiments. Actually, based on the following ultrafast dynamic analysis, this excitation enhancement of hot electrons may arise from the effective evacuation of conduction bands through ultrafast cooling of hot electrons.

III. ULTRAFAST DYNAMICS OF HOT ELECTRONS

To clarify the microscopic mechanism of unusual enhancement of the density of photoinduced hot electrons in heavily p-doped graphene by optical pumping, we
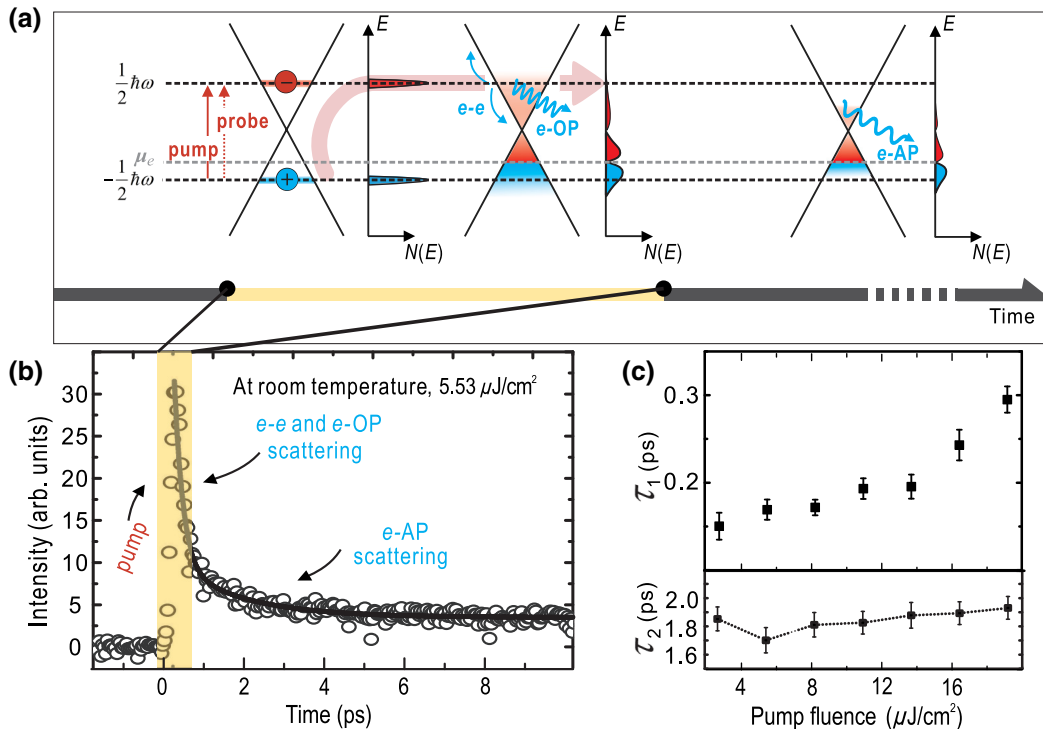

FIG. 2. (a) Schematic of the evolution of photoinduced hot carriers in heavily p-doped graphene after ultrafast optical excitation. The pump pulse creates a short-lived electron and hole distribution at energy levels of $\varepsilon = \pm 1/2 \hbar \omega$. The gray dashed line corresponds to the chemical potential μ_e of the heavily p-doped graphene. Then the hot electrons are cooled via fast (e-e and e-OP scatterings) and slower (e-AP scattering) decay processes, which are indicated by the blue arrows. (b) The corresponding measured transient differential reflection spectrum, placed at the same time axis as (a). The black solid curve is an analytical fit to the data using a biexponential function. (c) The fast decay time (τ_1) and slower decay time (τ_2) of SG under various pump fluences.

explore the evolution processes based on the time-domain photoinduced hot electron dynamics. As schematically illustrated in Fig. 2(a), during or immediately following the pulse duration τ_p of a 1.55-eV (800-nm) femtosecond laser pulse, a nonequilibrium population of hot electrons in the conduction band ($\varepsilon = 1/2\hbar\omega$) and holes in the valence band ($\varepsilon = -1/2\hbar\omega$) is created with momentum conservation. Specifically, by using a degenerate pump-probe setup, we can monitor the evolution of the hot-electron population at the specific energy level $\varepsilon = 1/2\hbar\omega$. The measured transient differential reflection spectrum is shown in Fig. 2(b). We describe the transient differential reflection signal with a model that includes a rise step and a biexponential decay step. In the excitation stage, the signal rise at a fixed value equals the pulse duration time τ_p (approximately 137 fs). After the peak, the hot electronic system then efficiently transfers energy as follows: (i) electron-electron (e-e) scattering governed by a strong Coulomb interaction at a time scale of approximately 30 fs [23,24,47], which is faster than our experimental time resolution, (ii) loss of energy to the lattice via electron-optical-phonon (e-OP) scattering within several hundred femtoseconds, and (iii) further cooling within several picoseconds via electron-acoustic-phonon (e-AP)

scattering [24]. Therefore, in a real cooling process, the transient differential reflection signal $I(t)$ can be fitted [as shown by the solid curve in Fig. 2(b)] by a biexponentially decaying function as [48]

$$I(t) = A_1 e^{-t/\tau_1} + A_2 e^{-t/\tau_2} + C, \qquad (4)$$

where $I(t)$ stands for the time-dependent signal of the cooling processes, τ_1 and τ_2 represent the fast and slower decay time constants, A_1 and A_2 are the contribution weights of the two decay processes, respectively, and C is a constant. Consistent with the discussions above, the fast decay time τ_1 involves the combined effect of e-e and e-OP scattering, while the slower decay time τ_2 is assigned to e-AP scattering. By fitting all the curves in Fig. 1(d) with Eq. (4) and by convoluting with the laser pulses envelope, we can obtain both τ_1 and τ_2 at different pump fluences. As indicated in Fig. 2(c), τ_1 increases from approximately 150 to 300 fs when the pump power is increased from 2.74 to 19.18 μJ/cm^2 (upper panel), which is of the same order as the excitation time ($\tau_p \sim 137$ fs) for exciting an electron; whereas τ_2 remains almost constant at approximately 1.8 ps (lower panel).
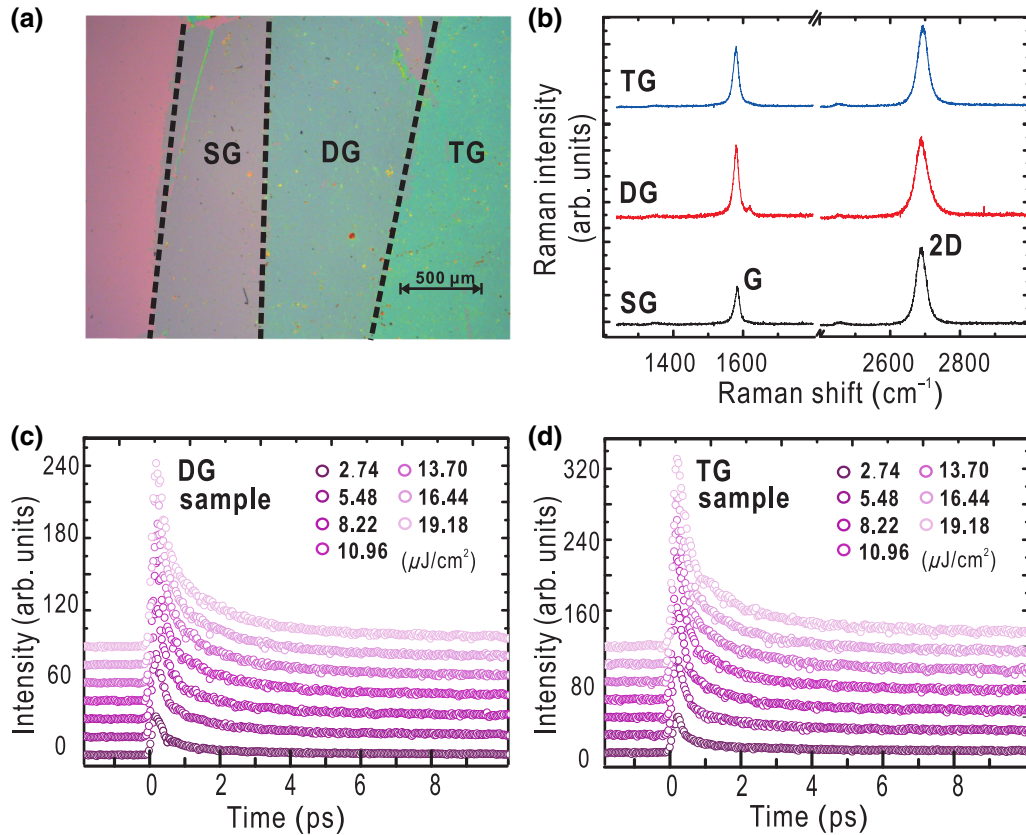

FIG. 3. (a) Optical image of layer-by-layer graphene stacks (SG, DG, and TG) transferred on SiO$_2$/Si substrate. (b) Raman spectra for differently stacked graphene layers. Black, red, and blue curves represent SG, DG, and TG, respectively. (c),(d) The measured transient differential reflection signal versus delay time plotted when increasing the pump fluence from 2.74 to 19.18 μJ/cm^2.

The experimental data show that the electron excitation and the cooling through fast-decay channel occur at the same time scales as highlighted by the yellow region in Fig. 2(b), specifically at low pump powers. The associated physical process can be understood based on the following descriptions. When a femtosecond laser beam is incident on a sample, the electrons are pumped to the empty conduction band with energy level $\varepsilon = 1/2\hbar\omega$ during or immediately following the pulse duration τ_p. Then, the fast e-e and e-OP scatterings cool these hot electrons. This effectively evacuates the conduction band within the same time scale equal to τ_p. Consequently, the hot-electron ultrafast cooling process may affect the excitation process, and makes it possible for the enhancement of excitation of hot electrons in graphene. This enhancement exists until the band-filling effect becomes prominent at high pumping energies.

IV. STRENGTHENING OF THE EXCITATION ENHANCEMENT OF HOT ELECTRONS

To strengthen the enhancement of the excitation of hot electrons, we increase the number of hot electrons by introducing layer-by-layer graphene stacks, including double-stacked graphene layers (DG) and triple-stacked graphene layers (TG). Meanwhile, the number of hot electrons can be nearly doubled (or tripled) in DG (or TG) compared with the scenario of SG at the same pump power. Figure 3(a) shows an optical microscopic image of graphene stacks (SG, DG, and TG). Experimentally we can easily distinguish the sample thickness based on color because samples with different numbers of layers have different optical absorption characteristics. Figure 3(b) shows

the Raman spectra of graphene with different numbers of stacked layers. The prominent G band at approximately 1580 cm^{-1} and the 2D band at approximately 2680 cm^{-1} are clearly resolved for all the samples. As the number of graphene layers increases, the ratio between the 2D peak and G peak decreases, whereas the 2D peak remains symmetric and maintains the Lorentzian profile [49]. Thus it is indicated that each layer still maintains the integrity of SG, even after the stacking.

We carry out femtosecond optical pump-probe measurements on DG and TG samples as well. As the number of stacking layers increases, the signal intensity of the transient differential reflection increases given that more hot electrons participate in the ultrafast excitation and cooling processes. The corresponding transient differential reflection spectra are shown in Figs. 3(c) and 3(d), respectively. As shown, the spectra possess similar features to those obtained from SG in Fig. 1(d). The differences between N (i.e., the density of photoinduced hot electrons) and the linear limit N_L of DG and TG at different pump powers are illustrated in Fig. 4(a). These exhibit the same tendencies as that of SG. The density of photoinduced hot electrons becomes larger than the linear limits within a range of pump fluence [marked by the gray, red, and blue colors in Fig. 4(a)].

As illustrated in Fig. 4(b), the value of τ_1 increases as the pump fluence is increased, whereas τ_2 remains almost constant. The contribution weights of the fast decay (A_1) and slower decay (A_2) processes are plotted in Fig. 4(c). A_1 is much larger than A_2 at low pump power, thus suggesting that the channel for electron cooling is dominated by e-e and e-OP scattering at low pump power. As the pump power increases, A_1 of TG varies more rapidly. This
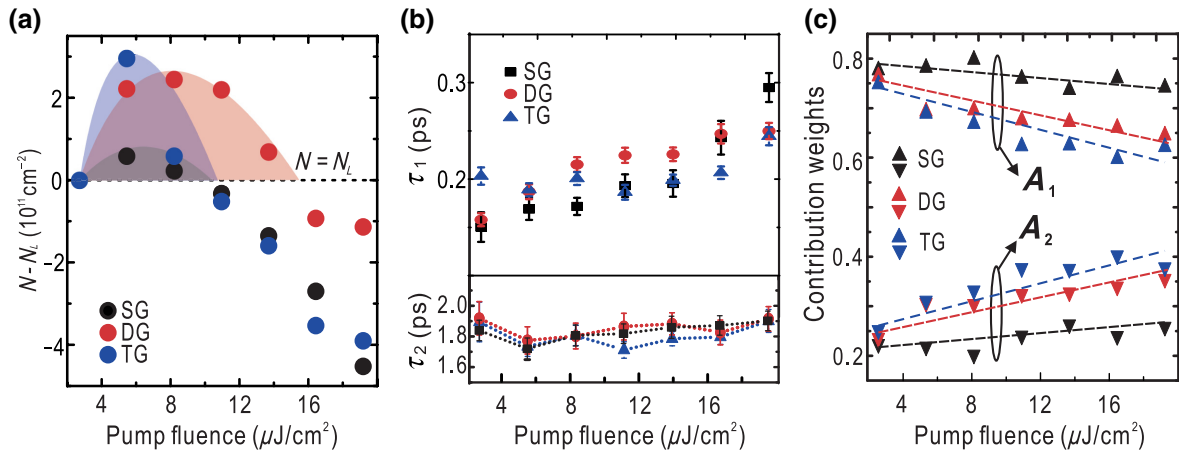

FIG. 4. (a) Pump fluence dependence of the difference between the density of photoinduced hot electrons (N) and its linear limit (N_L). The gray, red, and blue areas mark the regions where $N > N_L$ for graphene stacks (SG, DG, and TG, respectively), as a guide to the eye. (b) The fast decay time (τ_1) and the slower decay time (τ_2) are plotted with varying pump fluences in the upper and lower panels, respectively. Black, red, and blue represent graphene stacks (SG, DG, and TG, respectively). (c) The contribution weights in the fast decay process (A_1) and the slower decay process (A_2) are plotted at different pump powers. Black, red, and blue represent SG, DG, and TG, respectively.

corresponds to a more evident enhancement of the hot electrons.

An alternative approach to the enhancement of the ultra-fast cooling of hot electrons is to apply annealing pretreatment to samples. Recently, thermal annealing has been investigated as a common practice to eliminate contamination and restore clean surfaces of 2D materials, so that the annealed samples can attach more tightly on substrates [50]. Herein, we compare the density of the photoinduced hot electrons (N) and the electron cooling behaviors for graphene stacks with and without annealing. Two types of graphene samples are prepared: one is pristinely transferred to the substrate without any subsequent thermal treatment, whereas the other is annealed in an Ar-H_2 environment at 200 °C for 2.5 h. By applying a pump fluence of 5.48 μJ/cm^2, values of N of the annealed layer-by-layer graphene stacks (i.e., SG, DG, and TG) are rather larger compared to those of the pristine samples, as illustrated in Fig. 5(a). Moreover, the fast decay time τ_1 is shortened from approximately 230 to 200 fs [upper panel of Fig. 5(b)], and the slower decay time τ_2 is shortened from approximately 2.4 to 2.0 ps as well [lower panel of Fig. 5(b)]. Physically, annealing substantially reduces the charged impurities and eliminates structural disorders, and thus enhances the carrier mobility in graphene stacks [51–53]. We can infer that via the annealing process, both fast and slower decay times are effectively enhanced. Yet, according to our experimental data at different substrate temperatures, e-AP scattering (lasting for a few picoseconds) does not directly contribute to the hot-electron ultrafast evacuation of conduction bands in graphene (the details are given in the next section). With the use of annealing pretreatment, the fast decay time is shortened to a value that is closer to the time of the excitation process at the femtosecond level, which does help

to evacuate the conduction energy level quickly. All these results indicate that sample annealing pretreatment benefits the evacuation of the conduction bands, eventually leading to the additional enhanced density of the photoinduced hot electrons.

V. THE INFLUENCE OF ELECTRON-ACOUSTIC-PHONON SCATTERING

To investigate the possible influences of e-AP interaction on the excitation enhancement in graphene stacks, we measure the transient differential reflection of graphene stacks at different temperatures. Before that, we examine the characteristics of samples at different temperatures by Raman spectral measurements. As shown in Fig. 6, the Raman spectra are collected only when the substrate temperature is varied in monolayer graphene. As the substrate temperature increases from 30 to 130 °C, the G peaks change position from 1583.3 to 1581.2 cm^{-1} and the 2D peaks from 2687.6 to 2684.3 cm^{-1}. All Raman peaks broaden and their intensities decrease, which suggests that the behavior of acoustic phonons has been changed in the sample.

The abnormal transient differential reflection spectra of graphene stacks are measured at a pump fluence of 5.48 μJ/cm^2 while all other parameters are fixed, as shown in Fig. 7(a). This shows that the peak intensity is maintained almost the same as the temperature increases. This means that the density of the photoinduced hot electrons at different temperatures does not change significantly when the temperature increases. By fitting the curves of the transient differential reflection with the method discussed above, we obtain the temperature-dependent fast decay time τ_1 and slower decay time τ_2. We find that the fast decay time, τ_1, remains almost constant at different temperatures [upper
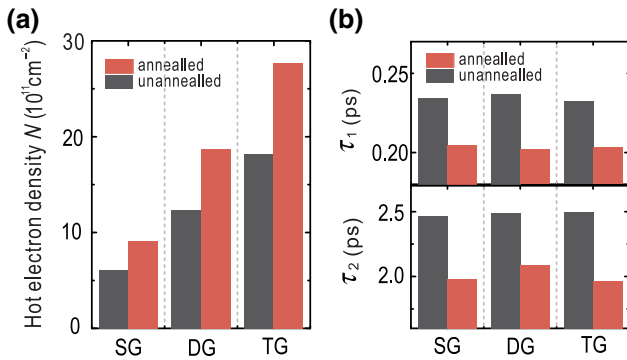

FIG. 5. (a) The photoinduced hot-electron density of graphene stacks (SG, DG, and TG) under a pump fluence of 5.48 μJ/cm^2 before or after annealing in an Ar-H_2 environment at 200 °C for 2.5 h. (b) Upper panel: the fast decay time (τ_1) of graphene stacks (SG, DG, and TG) before or after annealing. Lower panel: the slower decay time (τ_2) of graphene stacks (SG, DG, and TG) before or after annealing.
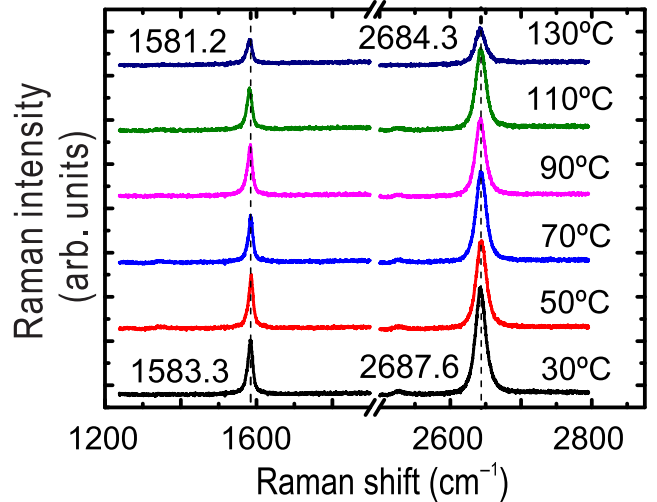

FIG. 6. Raman spectra measured for monolayer graphene with increasing temperature, illustrated using different colors.
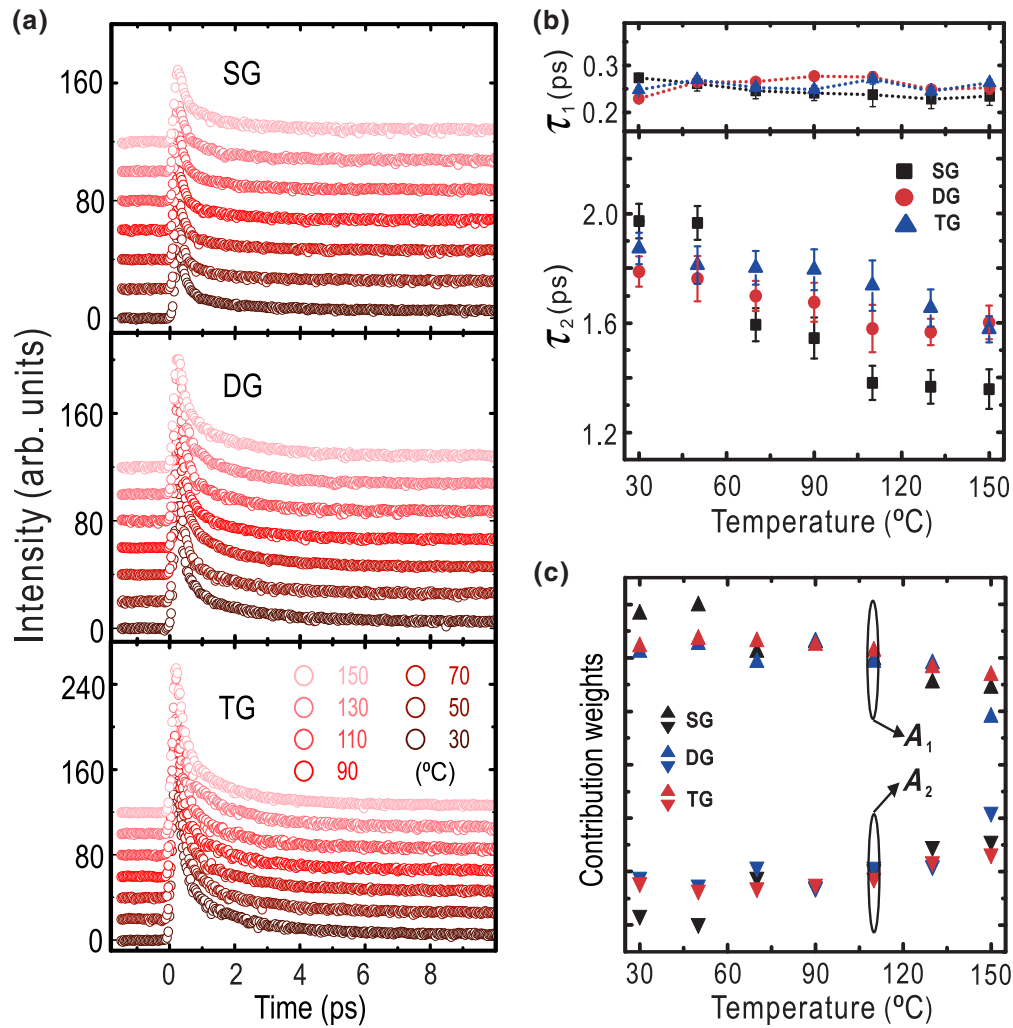
FIG. 7. (a) The measured normalized transient differential reflection signal versus delay time when varying the substrate temperature from 30 to 150 °C under a pump fluence of 5.48 μJ/cm^2. The curves are shifted for clarity. (b) The fast (τ_1) and slower (τ_2) decay times under a pump fluence of 5.48 μJ/cm^2 while varying the substrate temperature of graphene stacks (SG, DG, and TG). (c) The contribution weights versus substrate temperature of graphene stacks (SG, DG, and TG).

panel of Fig. 7(b)]. In contrast, the slower decay time, τ_2, decreases when the substrate temperature is increased from 30 to 150 °C [lower panel of Fig. 7(b)]. This corresponds to the temperature-dependent Raman spectrum. The contribution weights of graphene stacks are slightly changed as the temperature increases, as shown in Fig. 7(c). Based on the results described above, the slower *e*-AP scattering (which lasts for a few picoseconds) does not directly contribute to the ultrafast evacuation of hot electrons from the conduction bands in graphene stacks.

VI. ABSORPTION COEFFICIENTS AND MODULATION DEPTH

It is known that graphene shows remarkable optical properties, and it has an optical absorption of $\pi\alpha \approx 2.3\%$ over the entire visible spectrum [14], where α is the

fine-structure constant. The broad operating spectral range and ultrafast response are responsible for the potential of graphene-based photodetectors and optical modulators.

Here we pay attention to the absorption coefficients of the graphene stacks in our experiments. At a given pump intensity, the absorption coefficient of the sample satisfies $\alpha(I) = N(I) \times \hbar\omega_{\text{pump}}/I$, where I represents the pump intensity, $N(I)$ is the density of photoinduced hot electrons at different excitation intensities [see Eq. (3) in Sec. II], and $\hbar\omega_{\text{pump}} = 1.55$ eV in our experiments. As shown in Fig. 8(a), the absorption coefficient $\alpha(I)$ of monolayer graphene obviously surpasses the linear limit $\alpha_0 \cong 1.95\%$ below the threshold of approximately 11 μJ/cm^2. As for DG and TG, the absorption coefficients are illustrated in Fig. 8(b) at different pump fluence, which exhibit a similar tendency to that of SG. Moreover, as the stacking layers increase, the absorption coefficient shows a more evident
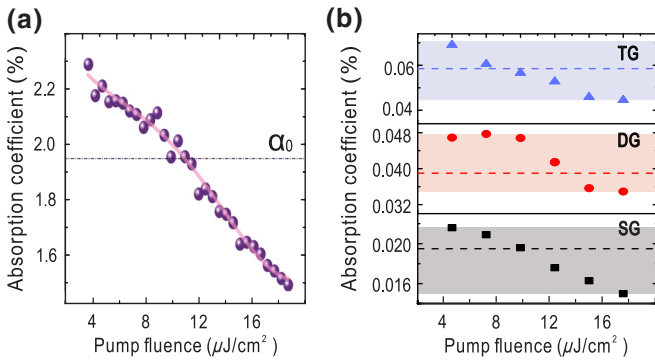
FIG. 8. (a) The absorption coefficients of SG from experimental data in Fig. 1(d). The linear limit of absorption coefficient α_0 for SG is marked by the dashed line. (b) Pump fluence dependence of the absorption coefficients for SG, DG, and TG in black, red, and blue, respectively. The linear absorption coefficients for SG, DG, and TG are marked by dashed lines with corresponding colors.

enhancement, especially at low pump fluence. This means that we achieve an increased absorption, especially at low excitation energy.

The modulation depth, i.e., $\Delta\alpha = |\alpha(I_{\min}) - \alpha(I_{\max})|$, describes the extent of the variation of the modulated signal with respect to its unmodulated level, and can be regarded as the relative maximum change in the absorption coefficient. In our experiments, $I_{\min}$ is 2.74 μJ/cm^2 and $I_{\max}$ is 19.18 μJ/cm^2. According to Fig. 8, $\Delta\alpha$ of SG can reach approximately 0.79% for a small pump-fluence change ($< 20 \ \mu$J/cm^2), and further increases to approximately 1.2% and approximately 2.5% for DG and TG, respectively. These outcomes are better than those reported in previous studies, for example, which yielded $\Delta\alpha$ of 1.8% when reaching very high saturation fluence of 180 μJ/cm^2 [54] in three-layer graphene near 1550 nm. This large modulation depth in our highly doped graphene stacks indicates that the absorption of graphene stacks can be sufficiently altered by an extremely small variation of pump fluence, and will be favorable for high-speed optical modulators and efficient light harvesting.

VII. CONCLUSIONS

In conclusion, we have demonstrated here the enhanced excitation of hot electrons in heavily p-doped graphene stacks with ultrafast weak optical pumping, where both carrier multiplication and population inversion are suppressed. Degenerate ultrafast pump-probe experiments are carried out to observe the depletion (increase) of carrier intensity around the energy of the initial states of the excitation at a femtosecond time scale. For relatively long-pulse excitations, the time scale for electron excitation is proven to be of the same order as that of electron cooling through e-e and e-OP scatterings. Therefore, the

excitation of hot electrons may be significantly enhanced owing to the fast cooling of hot electrons. By introducing layer-by-layer graphene stacks and applying annealing pretreatment, we manage to further enhance the excitation of hot electrons in graphene. Owing to the excitation enhancement of hot electrons, the optical absorption of graphene stacks is increased with an extremely low threshold of pump fluence ($<20 \ \mu$J/cm^2), which suggests that the heavily p-doped graphene stacks can maximize the number of hot electrons, especially in a low-fluence situation. A large modulation depth is also achieved in graphene stacks, indicating that the absorption can be sufficiently altered with an extremely small variation of pump fluence. These results expand the applicability of graphene for efficient light harvesting and high-speed optical modulators. Despite the fact that this enhancement effect is observed here in graphene stacks, we can expect that it is not restricted to graphene-based systems only, and it may occur in other natural or artificial materials with simple energy-level schemes, relatively long-pulse excitation and ultrafast decay dynamics. We anticipate that these investigations may provide valuable perspectives for exploring alternative hot-electron-driven photoelectrical and photochemical phenomena, and provide unique ways to achieve high-speed ultrathin hot-electron devices.

[1] M. L. Brongersma, N. J. Halas, and P. Nordlander, Plasmon-induced hot carrier science and technology, Nat. Nanotechnol. **10**, 25 (2015).

[2] A. J. Nozik, Utilizing hot electrons, Nat. Energy **3**, 170 (2018).

[3] H. N. Barad, A. Ginsburg, H. Cohen, K. J. Rietwyk, D. A. Keller, S. Tirosh, Y. Bouhadana, A. Y. Anderson, and A. Zaban, Hot electron-based solid state TiO$_2$|Ag solar cells, Adv. Mater. Interfaces **3**, 1500789 (2016).

[4] N. M. Gabor, J. C. Song, Q. Ma, N. L. Nair, T. Taychatanapat, K. Watanabe, T. Taniguchi, L. S. Levitov, and P. Jarillo-Herrero, Hot carrier-assisted intrinsic photoresponse in graphene, Science **334**, 648 (2011).

[5] H. Chalabi, D. Schoen, and M. L. Brongersma, Hot-electron photodetection with a plasmonic nanostripe antenna, Nano Lett. **14**, 1374 (2014).

[6] W. Li and J. Valentine, Metamaterial perfect absorber based hot electron photodetection, Nano Lett. **14**, 3510 (2014).

[7] V. R. Holm, B. Y. Zheng, P. M. Denby, B. Holst, N. J. Halas, and M. M. Greve, Work function-driven hot electron

extraction in a bimetallic plasmonic MIM device, ACS Photon. **5,** 1202 (2018).

[8] S. Mukherjee, F. Libisch, N. Large, O. Neumann, L. V. Brown, J. Cheng, J. B. Lassiter, E. A. Carter, P. Nordlander, and N. J. Halas, Hot electrons do the impossible: Plasmon-induced dissociation of H_2 on Au, Nano Lett. **13,** 240 (2013).

[9] Y. Zhang, S. He, W. Guo, Y. Hu, J. Huang, J. R. Mulcahy, and W. D. Wei, Surface-plasmon-driven hot electron photochemistry, Chem. Rev. **118,** 2927 (2018).

[10] K. Wu, J. Chen, J. R. McBride, and T. Lian, Efficient hot-electron transfer by a plasmon-induced interfacial charge-transfer transition, Science **349,** 632 (2015).

[11] W. A. Tisdale, K. J. Williams, B. A. Timp, D. J. Norris, E. S. Aydil, and X.-Y. Zhu, Hot-electron transfer from semiconductor nanocrystals, Science **328,** 1543 (2010).

[12] M. L. Mueller, X. Yan, B. Dragnea, and L.-S. Li, Slow hot-carrier relaxation in colloidal graphene quantum dots, Nano Lett. **11,** 56 (2011).

[13] K. S. Novoselov, A. K. Geim, S. V. Morozov, D. Jiang, Y. Zhang, S. V. Dubonos, I. V. Grigorieva, and A. A. Firsov, Electric field effect in atomically thin carbon films, Science **306,** 666 (2004).

[14] K. S. Novoselov, V. I. Fal'ko, L. Colombo, P. R. Gellert, M. G. Schwab, and K. Kim, A roadmap for graphene, Nature **490,** 192 (2012).

[15] S. Z. Butler, S. M. Hollen, L. Cao, Y. Cui, J. A. Gupta, H. R. Gutiérrez, T. F. Heinz, S. S. Hong, J. Huang, A. F. Ismach, *et al.*, Progress, challenges, and opportunities in two-dimensional materials beyond graphene, ACS Nano **7,** 2898 (2013).

[16] M. Xu, T. Liang, M. Shi, and H. Chen, Graphene-like two-dimensional materials, Chem. Rev. **113,** 3766 (2013).

[17] X. Liu, T. Galfsky, Z. Sun, F. Xia, E.-C. Lin, Y.-H. Lee, S. Kéna-Cohen, and V. M. Menon, Strong light-matter coupling in two-dimensional atomic crystals, Nature Photon. **9,** 30 (2015).

[18] J. Yan, M. H. Kim, J. A. Elle, A. B. Sushkov, G. S. Jenkins, H. M. Milchberg, M. S. Fuhrer, and H. Drew, Dual-gated bilayer graphene hot-electron bolometer, Nat. Nanotechnol. **7,** 472 (2012).

[19] Y. Kang, S. Najmaei, Z. Liu, Y. Bao, Y. Wang, X. Zhu, N. J. Halas, P. Nordlander, P. M. Ajayan, J. Lou, and Z. Fang, Plasmonic hot electron induced structural phase transition in a MoS_2 monolayer, Adv. Mater. **26,** 6467 (2014).

[20] Q. Ding, Y. Shi, M. Chen, H. Li, X. Yang, Y. Qu, W. Liang, and M. Sun, Ultrafast dynamics of plasmon-exciton interaction of Ag nanowire-graphene hybrids for surface catalytic reactions, Sci. Rep. **6,** 32724 (2016).

[21] Y. Yu, Z. Ji, S. Zu, B. Du, Y. Kang, Z. Li, Z. Zhou, K. Shi, and Z. Fang, Ultrafast plasmonic hot electron transfer in Au nanoantenna/MoS_2 heterostructures, Adv. Funct. Mater. **26,** 6394 (2016).

[22] I. Gierz, M. Mitrano, J. C. Petersen, C. Cacho, I. C. E. Turcu, E. Springate, A. Stöhr, A. Köhler, U. Starke, and A. Cavalleri, Population inversion in monolayer and bilayer graphene, J. Phys.: Condens. Matter **27,** 164204 (2015).

[23] I. Gierz, J. C. Petersen, M. Mitrano, C. Cacho, I. C. E. Turcu, E. Springate, A. Stöhr, A. Köhler, U. Starke, and A. Cavalleri, Snapshots of non-equilibrium Dirac carrier distributions in graphene, Nat. Mater. **12,** 1119 (2013).

[24] J. C. Johannsen, S. Ulstrup, F. Cilento, A. Crepaldi, M. Zacchigna, C. Cacho, I. C. E. Turcu, E. Springate, F. Fromm, C. Raidel, *et al.*, Direct View of hot Carrier Dynamics in Graphene, Phys. Rev. Lett. **111,** 027403 (2013).

[25] J. C. Johannsen, S. Ulstrup, A. Crepaldi, F. Cilento, M. Zacchigna, J. A. Miwa, C. Cacho, R. T. Chapman, E. Springate, F. Fromm, *et al.*, Tunable carrier multiplication and cooling in graphene, Nano Lett. **15,** 326 (2015).

[26] I. Gierz, F. Calegari, S. Aeschlimann, M. C. Cervantes, C. Cacho, R. T. Chapman, E. Springate, S. Link, U. Starke, C. R. Ast, and A. Cavalleri, Tracking Primary Thermalization Events in Graphene with Photoemission at Extreme Time Scales, Phys. Rev. Lett. **115,** 086803 (2015).

[27] E. Malic, T. Winzer, F. Wendler, S. Brem, R. Jago, A. Knorr, M. Mittendorff, J. C. König-Otto, T. Plötzing, D. Neumaier, H. Schneider, M. Helm, and S. Winnerl, Carrier dynamics in graphene: Ultrafast many-particle phenomena, Ann. Phys. (Berlin, Ger.) **529,** 1700038 (2017).

[28] F. Ceballos and H. Zhao, Ultrafast laser spectroscopy of two-dimensional materials beyond graphene, Adv. Funct. Mater. **27,** 1604509 (2017).

[29] D. Brida, A. Tomadin, C. Manzoni, Y. J. Kim, A. Lombardo, S. Milana, R. R. Nair, K. S. Novoselov, A. C. Ferrari, G. Cerullo, and M. Polini, Ultrafast collinear scattering and carrier multiplication in graphene, Nat. Commun. **4,** 1987 (2013).

[30] P. J. Hale, S. M. Hornett, J. Moger, D. Horsell, and E. Hendry, Hot phonon decay in supported and suspended exfoliated graphene, Phys. Rev. B **83,** 121404 (2011).

[31] D. Sun, G. Aivazian, A. M. Jones, J. S. Ross, W. Yao, D. Cobden, and X. Xu, Ultrafast hot-carrier-dominated photocurrent in graphene, Nat. Nanotechnol. **7,** 114 (2012).

[32] Q. L. Bao, H. Zhang, Y. Wang, Z. H. Ni, Y. L. Yan, Z. X. Shen, K. P. Loh, and D. Y. Tang, Atomic-layer graphene as a saturable absorber for ultrafast pulsed lasers, Adv. Funct. Mater. **19,** 3077 (2009).

[33] P. A. George, J. Strait, J. Dawlaty, S. Shivaraman, M. Chandrashekhar, F. Rana, and M. G. Spencer, Ultrafast optical-pump terahertz-probe spectroscopy of the carrier relaxation and recombination dynamics in epitaxial graphene, Nano Lett. **8,** 4248 (2008).

[34] T. Winzer, A. Knorr, M. Mittendorff, S. Winnerl, M.-B. Lien, D. Sun, T. B. Norris, M. Helm, and E. Malic, Absorption saturation in optically excited graphene, Appl. Phys. Lett. **101,** 221115 (2012).

[35] T. Winzer, M. Mittendorff, S. Winnerl, H. Mittenzwey, R. Jago, M. Helm, E. Malic, and A. Knorr, Unconventional double-bended saturation of carrier occupation in optically excited graphene due to many-particle interactions, Nat. Commun. **8,** 15042 (2017).

[36] M. Liu, X. Yin, E. Ulin-Avila, B. Geng, T. Zentgraf, L. Ju, F. Wang, and X. Zhang, A graphene-based broadband optical modulator, Nature **474,** 64 (2011).

[37] Y. Zhou, Y.-Q. Dong, R.-H. Fan, Q. Hu, R.-W. Peng, and M. Wang, Asymmetric transmission of terahertz waves through a graphene-loaded metal grating, Appl. Phys. Lett. **105,** 041114 (2014).

[38] J. Ye, M. F. Craciun, M. Koshino, S. Russo, S. Inoue, H. Yuan, H. Shimotani, A. F. Morpurgo, and Y. Iwasa, Accessing the transport properties of graphene and its multilayers

at high carrier density, Proc. Natl. Acad. Sci. USA **108,** 13002 (2011).

[39] W. Bao, Z. Fang, J. Wan, J. Dai, H. Zhu, X. Han, X. Yang, C. Preston, and L. Hu, Aqueous gating of van der Waals materials on bilayer nanopaper, ACS Nano **8,** 10606 (2014).

[40] K.-J. Tielrooij, J. Song, S. A. Jensen, A. Centeno, A. Pesquera, A. Z. Elorza, M. Bonn, L. Levitov, and F. Koppens, Photoexcitation cascade and multiple hot-carrier generation in graphene, Nature Phys. **9,** 248 (2013).

[41] M. Breusing, S. Kuehn, T. Winzer, E. Malić, F. Milde, N. Severin, J. P. Rabe, C. Ropers, A. Knorr, and T. Elsaesser, Ultrafast nonequilibrium carrier dynamics in a single graphene layer, Phys. Rev. B **83,** 153410 (2011).

[42] S. Wu, W.-T. Liu, X. Liang, P. J. Schuck, F. Wang, Y. R. Shen, and M. Salmeron, Hot phonon dynamics in graphene, Nano Lett. **12,** 5495 (2012).

[43] K. M. Dani, J. Lee, R. Sharma, A. D. Mohite, C. M. Galande, P. M. Ajayan, A. M. Dattelbaum, H. Htoon, A. J. Taylor, and R. P. Prasankumar, Intraband conductivity response in graphene observed using ultrafast infrared-pump visible-probe spectroscopy, Phys. Rev. B **86,** 125403 (2012).

[44] H. Shan, Y. Yu, X. Wang, Y. Luo, S. Zu, B. Du, T. Han, B. Li, Y. Li, J. Wu, *et al.*, Direct observation of ultrafast plasmonic hot electron transfer in the strong coupling regime, Light: Sci. Appl. **8,** 9 (2019).

[45] H. Choi, F. Borondics, D. A. Siegel, S. Y. Zhou, M. C. Martin, A. Lanzara, and R. A. Kaindl, Broadband electromagnetic response and ultrafast dynamics of few-layer epitaxial graphene, Appl. Phys. Lett. **94,** 172102 (2009).

[46] T. Plötzing, T. Winzer, E. Malic, D. Neumaier, A. Knorr, and H. Kurz, Experimental verification of carrier multiplication in graphene, Nano Lett. **14,** 5371 (2014).

[47] P. A. Obraztsov, M. G. Rybin, A. V. Tyurnina, S. V. Garnov, E. D. Obraztsova, A. N. Obraztsov, and Y. P. Svirko, Broadband light-induced absorbance change in multilayer graphene, Nano Lett. **11,** 1540 (2011).

[48] S. Kumar, M. Anija, N. Kamaraju, K. Vasu, K. Subrahmanyam, A. Sood, and C. Rao, Femtosecond carrier dynamics and saturable absorption in graphene suspensions, Appl. Phys. Lett. **95,** 191911 (2009).

[49] A. C. Ferrari, J. C. Meyer, V. Scardaci, C. Casiraghi, M. Lazzeri, F. Mauri, S. Piscanec, D. Jiang, K. S. Novoselov, S. Roth, and A. K. Geim, Raman Spectrum of Graphene and Graphene Layers, Phys. Rev. Lett. **97,** 187401 (2006).

[50] Z. Cheng, Q. Zhou, C. Wang, Q. Li, C. Wang, and Y. Fang, Toward intrinsic graphene surfaces: A systematic study on thermal annealing and wet-chemical treatment of SiO_2-supported graphene devices, Nano Lett. **11,** 767 (2011).

[51] J.-H. Chen, C. Jang, S. Adam, M. Fuhrer, E. Williams, and M. Ishigami, Charged-impurity scattering in graphene, Nature Phys. **4,** 377 (2008).

[52] K. Bolotin, K. Sikes, J. Hone, H. Stormer, and P. Kim, Temperature-Dependent Transport in Suspended Graphene, Phys. Rev. Lett. **101,** 096802 (2008).

[53] H. A. Hafez, X. Chai, Y. Sekine, M. Takamura, K. Oguri, I. Al-Naib, M. M. Dignam, H. Hibino, and T. Ozaki, Effects of environmental conditions on the ultrafast carrier dynamics in graphene revealed by terahertz spectroscopy, Phys. Rev. B **95,** 165428 (2017).

[54] J. Sotor, M. Pawliszewska, G. Sobon, P. Kaczmarek, A. Przewolka, I. Pasternak, J. Cajzl, P. Peterka, P. Honzátko, *et al.*, All-fiber Ho-doped mode-locked oscillator based on a graphene saturable absorber, Opt. Lett. **41,** 2592 (2016).